UNIVERSITY OF ŽILINA
FACULTY OF ELECTRICAL ENGINEERING

11th International Conference
ELEKTRO 2016
Štrbské Pleso - High Tatras

MAY 16 – 18, 2016
SLOVAK REPUBLIC

www.elektro.uniza.sk

PROCEEDINGS

TECHNICALLY CO-SPONSORED BY

region 8 IEEE

IEEE
Czechoslovakia Section

IAS
IEEE INDUSTRY APPLICATIONS SOCIETY
ICS
IAS/IES Joint Chapter
Czechoslovakia Section IEEE

University of Žilina
Faculty of Electrical Engineering

ELEKTRO²⁰¹⁶

11th International Conference

PROCEEDINGS

Organized By	Faculty of Electrical Engineering, University of Žilina, Slovak Republic
Sponsored By	Pow-en, a.s., Bratislava, SK
	VÚJE, a.s., Trnava, SK
	IBM Slovensko, s.r.o., Bratislava, SK
	ASBIS SK, s.r.o., Bratislava, SK
	Orange Slovensko, a.s., Bratislava, SK
	Eltek, s.r.o., Liptovský Hrádok, SK
	KVANT, s.r.o., Bratislava, SK
	Panasonic Industrial Devices Slovakia, s.r.o., Trstená, SK
	Marpex, s.r.o., Dubnica nad Váhom, SK
	NXP Semiconductors Czech Republic s.r.o., Rožnov pod Radhoštěm, CZ
	Tepláreň, a.s., Považská Bystrica, SK
	HUMUSOFT, s.r.o. - Praha, CZ
Technical Co-Sponsorship	Czechoslovakia Section of IEEE
	IEEE Region 8
	IAS/IES joint chapter of Czechoslovakia section, IEEE
In Cooperation With	Advances in Electrical and Electronic Engineering
Conference Bureaus	KAP, Alumni Club of Faculty of Electrical Engineering
Conference Website	http://www.elektro.uniza.sk
Conference E-mail Address	elektro@fel.uniza.sk
Published By	Faculty of Electrical Engineering, University of Žilina, Univerzitná 8215/1, 010 26 Žilina, Slovak Republic
Edited By	Peter Brida, Jozef Dubovan, Miroslav Markovič
Front Cover Design	Jozef Dubovan
Printed By	Faculty of Electrical Engineering, University of Žilina, Univerzitná 8215/1, 010 26 Žilina, Slovak Republic

Frequency Control in Smart Grids Based on Renewables vs. ENSTO-E Grid Code Requirements

Martina Latkova, Peter Bracinik, Michal Bahernik
Department of Power Electrical Systems
Faculty of Electrical Engineering, University of Zilina
Zilina, Slovak Republic
martina.latkova@kves.uniza.sk

Sandra Krollova
Air Transport Department
Faculty of Operation and Economics of Transport and
Communications, University of Zilina
Zilina, Slovak Republic

Abstract— **The paper presents the operation and frequency control in the Smart Grid region during overfrequency. The studied region consists of a PV power plant, a conventional source represented by a small synchronous generator with the speed controller and a load. The frequency control defined by the recent ENTSO-E Grid Code for generating units of type B is applied on the PV power plant operation and the influence of such control on frequency changes is studied. Obtained simulation results are used to outline a possible solution for future Smart Grid regions' frequency control.**

Keywords—frequency control; Smart Grids, renewables, Grid Code

I. INTRODUCTION

The future of electric networks is more and more connected with the Smart Grid concept. The term Smart Grid covers more than only one feature. It should help to improve the operation of electric networks, bring benefits both for electricity suppliers and consumers and lead to the fulfillment of goals defined by the directive 2009/28/EC.

One of the most discussed and promising Smart Grid features is the covering of local demand by a local electricity generation being provided by distributed generation consisting mainly of renewable energy sources (RESs). Such application of RESs brings a lot of changes to their operation, especially in the field of frequency control. The frequency control, being previously provided by big conventional power plants on power transmission level, should be now transferred to RESs, the sources with an intermittent generation and a strong dependence on weather conditions.

However, a lot of control strategies enabling RESs to provide the frequency control have been designed by the scientific community so far. Generally, they can be divided among three following groups. The first group of control strategies is based on the use of frequency droop algorithms, either applied directly in the MPPT control of primary DC source [1], [2], [3] or in the network tied inverter [4]. Algorithms in the second group add some energy balance mechanism to the RESs operation. It is usually a load shedding [5] or a combination with battery energy storage systems (BESS) [6], [7]. The last group of control strategies is based on the combination of one or both previous ones with some kind of a prediction, based either on multi agent systems or genetic algorithms [8], [9] or on a weather prediction [10].

The majority of proposed control strategies were developed and tested on sources with a small output, from 2 to 48 MW, which are expected to be sufficient for feeding a specific part/region of the Smart Grid (nowadays more represented by micro grids). Unfortunately, in most cases, the authors did not take care of regulations for electricity generators specified in valid grid codes, e.g. ENTSO-E Grid Code, which specify the regulations for the frequency control as well.

It does not mean, that designed control algorithms are wrong. They only do not meet valid legislation regulations. So a question arises, what should be changed in the future – the algorithms or requirements for generators in grid codes? This paper introduces a possible answer for this question, based on the simple simulation of an overfrequency case in a small Smart Grid region consisting of a photovoltaic power plant, a diesel generator and a local load.

Firstly, the ENTSO-E requirements relevant to the analyzed problem will be pointed out in Section II. Then a short summary of RESs control capabilities will be given in Section III. Section IV will be devoted to the description of the used study case and its simulation model as well. Obtained simulation results will be presented and analyzed in Section V. The last Section of this paper will be devoted to conclusions as well as to the outline of future work.

II. APPROPRIATE ENTSO-E REQUIREMENTS

As many of RESs need an inverter interface in order to export power to a 50 Hz distribution network, they are classified as Power Park Modules (PPM) according to the recent version of Requirements for Generators part (NC RfG) of the ENTSO-E Grid Code [11].

Power park module (PPM) is a unit or ensemble of units generating electricity, which is either non-synchronously connected to the network or connected through power electronics, and that also has a single connection point to a transmission system, distribution system including closed distribution system or HVDC system [11].

As it was mentioned above, the expected power output of RESs feeding smart regions/micro grids varies from 2 MW to 48 MW. The NC RfG classifies such PPMs working in the

Continental Europe as generating units of the type B (with the maximum installed capacity under 50 MW), that should be capable of remaining connected to the network and operate within the frequency ranges 49.0 – 51.0 Hz. Moreover, if needed, they shall be capable of activating the provision of active power frequency response according to the Fig. 1. Such operation is called limited frequency sensitive mode - overfrequency (LFSM-O). The frequency point ($|\Delta f_1|/f_n$), at which the PPM's output should start to follow defined droop, can be set by the Transmission System Operator (TSO) between 50.2 – 50.5 Hz. The droop settings shall be between 2 % and 12 % [11].
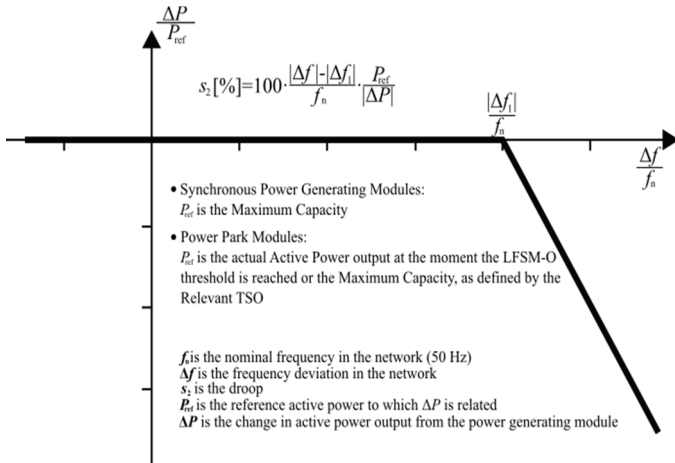
Fig. 1. Active power frequency response capability of power generating modules in LFSM-O mode

III. RESs' CONTROL CAPABILITIES

The RESs control strategy capabilities mainly include a maximum power point tracking (MPPT) control strategy, a storage battery charging and discharging control strategy (if equipped with the storage battery), an inverter control strategy and a network control strategy.

A. MPPT control

Renewables utilizing a wind or a solar irradiance as a prime source of their energy are usually operated at their instantaneous maximum power point (MPP) in order to achieve the maximum system output and so improve the system power efficiency. Nowadays, there are a lot of methods how to reach the MPP (MPPT). Methods used in photovoltaic systems are the constant-voltage method, the electric conductance incremental method, the disturbance of observation, the hysteresis comparison method, the optimal gradient method, the fuzzy logic control method and the artificial neural network intelligent control method, etc. The control is usually done at the DC converter level, where the MPPT controller changes the duty cycle of the converter to achieve the maximum power point [12].

B. Inverter Control

Due to the very large variety of PV inverter topologies used in RESs systems, the applied control structures are also very different. The modulation algorithm has to be specific for each topology [13].

Basic functions (common for all grid connected inverters) are a grid current control, a DC voltage control and a grid synchronization. The grid current control tries to meet the THD limits imposed by standards and ensures the stability in the case of large grid impedance variations. The DC voltage control does the adaptation to grid voltage variations and the grid synchronization ensures the operation at the unity power factor as required by standards. All three functions provide ride-through grid voltage disturbances [13].

C. Network Control

The network control is carried out according to the grid code established for the specific TSO's responsibility area.

IV. STUDY CASE

A study case was created in order to analyse the influence of valid legislative requirements, represented by the grid codes of Slovak TSO and ENTSO-E, on the RESs ability to provide the frequency control in the Smart Grid region at overfrequency. A created simulation model, consisting of the power park module represented by photovoltaic power plant (PV), a synchronous power generating module represented by a diesel generator (SG) and a local load (Load) is shown in Fig. 2. The voltage level of the system is 22 kV.
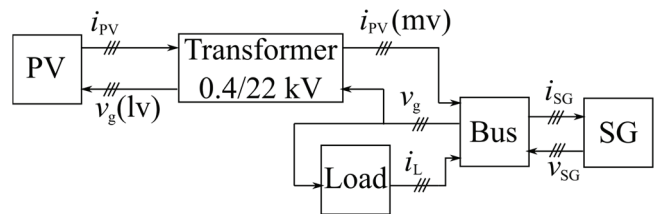
Fig. 2. Simulation case block diagram

A. Model of Synchronous Power Generating Module

The synchronous power generating module is represented by the diesel generator with the nominal output 2.5 MW (SG). Its simulation model is represented by a swing equation [14]:

$$\frac{d\omega_m}{dt} = \frac{1}{J \cdot \omega_m}\left(P_m - P_e\right), \tag{1}$$

where ω_m is the mechanical speed of the rotor (in case of 2 pole's machine $\omega_m = \omega_e$), J is the inertia of the synchronous generator (SG), P_m and P_e are the mechanical and electrical power of the SG, respectively.

The SG has the constant output voltage but it is equipped with a speed control system, which consists of a PI regulator. The control of speed is implemented within the range of 70 – 100 % of the SG rated power (1.75 – 2.5 MW).

B. Model of Power Park Module

The power park module is represented by the model of photovoltaic (PV) power plant (1 MW) consisting of mathematical models of a PV array, a DC boost converter with a maximum power point tracking (MPPT) controller and a voltage source converter (VSC) with a phase locked loop controller (PLL) (Fig. 3). The PV array, the DC boost converter and the MPPT controller are more described in [15].

The inputs of the PV array model are a solar irradiance λ, an air temperature T and a load current I from the DC boost converter. They are used to calculate the PV array voltage V that is used as an input for the model of DC boost converter and the PV array open circuit voltage V_{OC} that is used in the MPPT controller. The DC boost converter calculates the increased output voltage V_{DC} and the load current I.

The switching of the DC boost converter is controlled by the MPPT controller, which changes its duty cycle D according to the voltage from the PV array and the open circuit voltage of the PV array. The MPPT controller´s algorithm determines the duty cycle needed to operate the PV array in a point of its maximum power.
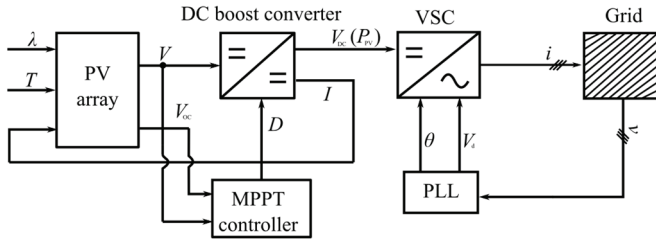
Fig. 3.   Block diagram of the PV power plant model.

The increased voltage V_{DC} from the DC boost converter (to simplify inverter's modelling an array's power P_{PV} is used instead), together with phase angle θ and the amplitude of the grid voltages V_d from the PLL, is consequently used in the voltage source converter for the three phase currents i determination. The phase angle and the amplitude of the grid voltages is identified from the grid voltage using the phase locked loop algorithm.

The VSC is represented by the Northon equivalent using dq0 transformation [16]. Assuming that the PV power plant should operate at a unity power factor and at maximum power point of the PV array, the current injected to the grid would be only for the active power and so the amplitude of the output current is:

$$I_G = I_d = \frac{2 \cdot P_{MPP}}{3 \cdot V_d}, \tag{2}$$

where V_d is the direct-axis projection of the grid voltage defining the amplitude of the voltage, I_d is the direct-axis projection of the source current defining its amplitude and P_{MPP} is the maximum power of the PV array.

An inverse Park transformation and phase angle from the phase-locked loop algorithm are then used to convert the current I_d to the three-phase current system.

The ability of LFSM-O operation has been added to the PV power plant model, with the frequency threshold set to 50.2 Hz and droop value equal to 5 %, with respect to definitions required in [11] and shown in Fig. 1. So the decreasing of the PV power plant output (PPM) was defined as [11]:

$$\Delta P = 20 \cdot P_m \frac{50.2 - f_{network}}{50.0}, \tag{3}$$

where ΔP is the power reduction and $f_{network}$ is the actual grid frequency.

C. Model of the Load

The model of local demand is represented by the impedance to the bus voltage. The power demand varies from 2.4 MW to 2.2 MW during the simulation in order to simulate the overfrequency in the modelled Smart Grid region.

V. SIMULATION RESULTS

The performance of simulation model was checked at normal operation conditions first [17]. Then a demand drop resulting in overfrequency was applied to test the frequency control in the Smart Grid region. The testing was done for two cases. In the first case, the LFSM-O operation of PV power plant (PPM) was not applied and it operated only within the frequency range $\Delta f < \pm 200$ mHz. Such operation is in accordance with the ENTSO-E Grid Code requirements for generators of the type B and is also required by the Slovak TSO. In the other case, the PV power plant decreased its output according (3) and Fig. 1.

A. Normal Operation

The output of PV power plant changes according to the changes of solar irradiance's value (Fig. 4). The synchronous power generating module (diesel generator) also changes its output within its pre-set regulation range and according to its droop characteristic. Since the power demand stays constant during the first five seconds, the changes of PV power plant generation are compensated by the frequency control of the diesel generator (SG). The comparison of load demand (Pload), the PV power plant output (Ppv) and the diesel generator output (Psg) during the normal operation is shown in Fig. 5.
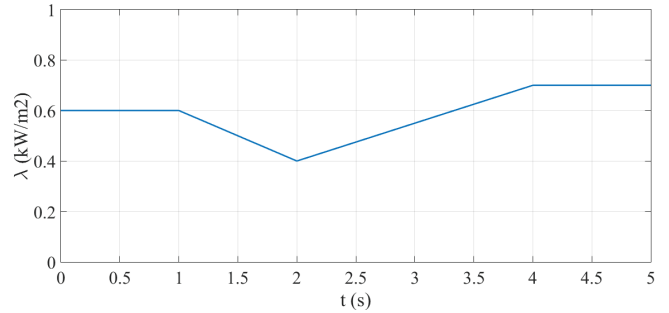
Fig. 4.   Changes of solar irradiance
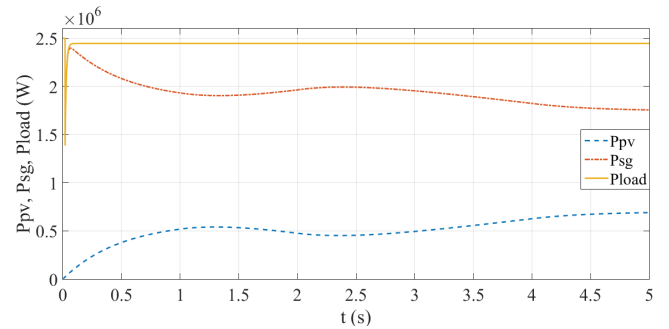
Fig. 5.   Power balance in the Smart Grid region during the normal operation

B. Overfrequency without the LFSM-O Activation

The operation of power generating unit during the overfrequency is defined by the grid code of a local TSO. If the

LFSM-O operation is not required for RESs, the TSO should define rules for RESs' operation at overfrequencies.

For example, the Slovak TSO defines in its grid code that a PV power plant has to be disconnected from the network, if the frequency exceeds 50.2 Hz [18].

To test such an operation of Smart Grid region, the decrease of demand from 2.4 to 2.2 MW was modeled (Fig. 6).
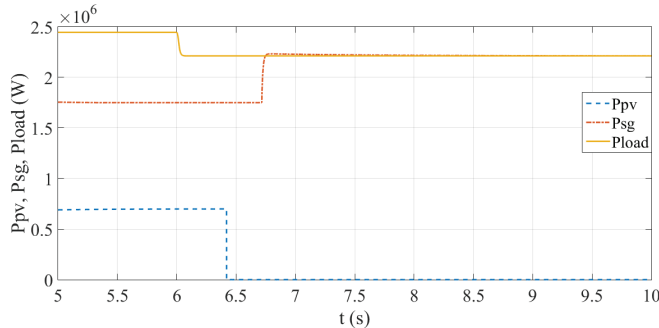
Fig. 6. The result of demand's change without LFSM-O activation

Because the output of PV power plant stays constant (since the value of solar irradiance did not change and the frequency is lower than 50.2 Hz) and the diesel generator is operating on its minimum regulation limit, the frequency of the Smart Grid region starts to rise (Fig. 7). When it reaches the value 50.2 Hz, the PV power plant is automatically disconnected (Fig. 6), what results in the change of power balance within the Smart Grid region, represented by the frequency drop (Fig. 7). When the frequency falls down under 50.0 Hz, the diesel generator increases its output, as shown in Fig. 6 (according its droop characteristic), in order to return the frequency to the nominal value (Fig. 7).
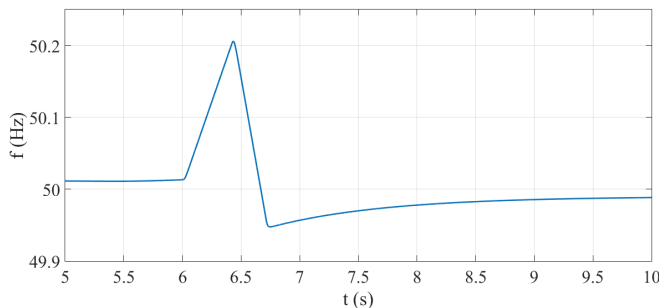
Fig. 7. Frequency's changes due to the PV power plant disconnection

Such operation looks to be good for the region. Unfortunately, when the nominal frequency is reached, there is no reason for the PV power plant to stay disconnected. So, when it is reconnected again, e.g. after some time delay or at dispatcher's command, and the region's demand does not change, the situation presented by Fig. 6 and Fig. 7 will repeat, thus resulting in cycles of PV power plant disconnections and reconnections (Fig. 8).

These repeated frequency changes could result in frequency oscillations. An example of such oscillations can be seen in Fig. 9, which was recorded at Duisburg training centre during the studies of generator behaviour during extreme states or faults in the electrical system. Fig. 9 shows frequency vibrations in the TenneT system caused by repeating one-minute reconnecting cycles of the PV power plant with the installed capacity more than 1 000 MW. This effect is possible in the regions with large installed power capacity of the power park modules and it is very dangerous.
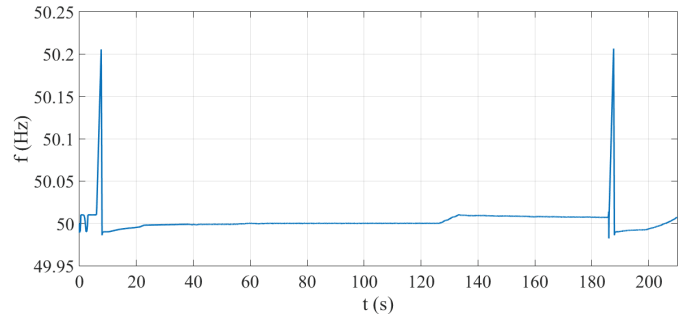
Fig. 8. Cycles of frequency changes caused by PV power plant reconnections
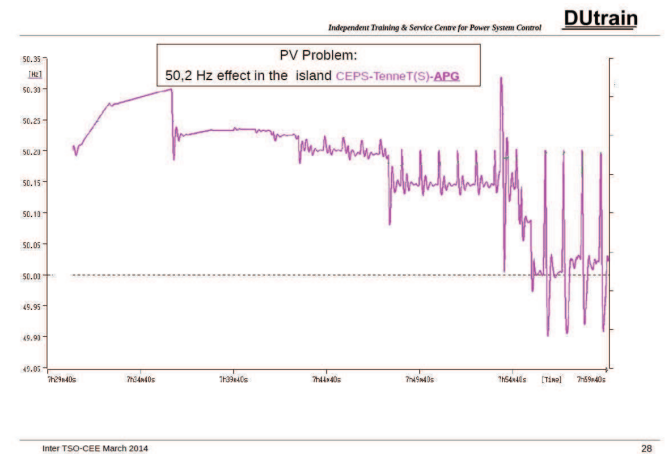
Fig. 9. Frequency vibrations in the TenneT system

C. Overfrequency with the LFSM-O Activation

If the LFSM-O operation is activated for the PV power plant at overfrequency, the PV power plant changes its output according the Fig. 1 and equation (3).

If the same situation, as in previous simulation case, is applied, the PV power plant generate a constant output up to the frequency 50.2 Hz. Then it decreases its output (Fig. 10) according the defined droop and the frequency deviation. The value, at which the frequency is stabilized, is given by the achieved power balance between generation and demand in the Smart Grid region.

The frequency in our simulation case is stabilized at the value bigger than 50.2 Hz (Fig. 11). Since the PV power plant remains connected, the frequency oscillations are neglected. However, the frequency deviation is too big and some actions needs to be done in order to restore the nominal frequency. Because the diesel generator operates on its minimum regulation limit and the output of the PV power plant is defined by frequency deviation, the regulation action has to be done through

auxiliary services provided either by the load (load shedding) or the main grid.
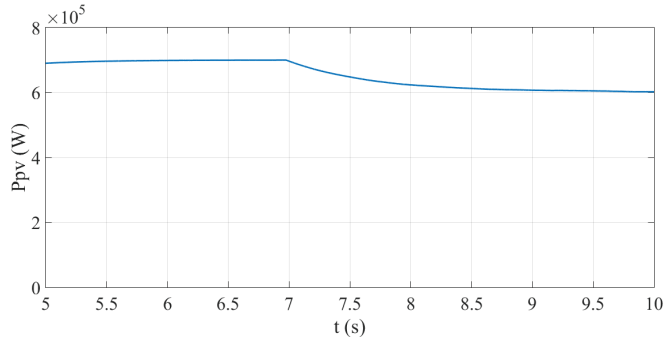
Fig. 10. The output of the PV power plant during LFSM-O operation
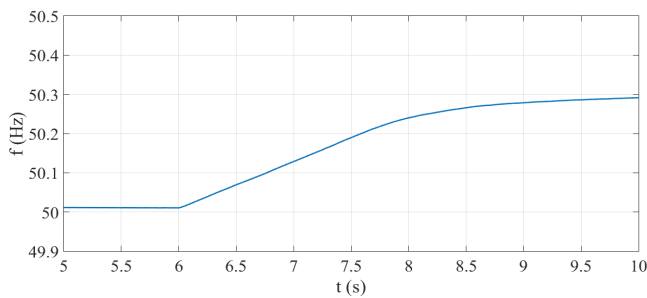
Fig. 11. The frequency of Smart Grid region after the LFSM-O activation

Despite the frequency stabilisation and frequency oscillations' elimination, the frequency deviation in the Smart Grid region is still too big. If the load shedding or the help of the main grid would not be possible, the generation units, including PPMs represented by the PV power plant, could not ensure the required quality of frequency control. A possible solution is the application of control features required for bigger generating units (type C or D).

VI. CONCLUSIONS

Installed capacity of renewable energy sources (PV power plant) mentioned to feed smart regions/microgrids usually varies from 2 MW to 48 MW. Such sources are classified, according to the valid ENSTO-E Grid Code, as generating units of type B. The way of their operation at frequencies bigger than 50.2 Hz has to be defined by the local TSO.

If they are disconnected and then repeatedly connected, when a system frequency returns bellow 50.2 Hz, it may result in repeating frequency oscillations with the negative influence on smart grid/microgrid operation.

If the LFSM-O mode is required by the TSO, the frequency oscillations can be neglected and the frequency can be stabilized. However, its value can be higher than 50.2 Hz. It strongly depends on the power balance in the given smart grid/microgrid. If so, some other actions should be applied to restore the frequency within allowed limits. Hence the application of requirements defined for bigger generating units (e.g. type C), based on the droop characteristics, should be considered for application in RESs based power park modules.

REFERENCES

[1] V.A.K. Pappu, B. Chowdhury, R. Bhatt, "Implementing frequency regulation capability in a solar photovoltaic power plant", *North American Power Symposium (NAPS)*, IEEE, pp. 1-6, September 2010, ISBN 978-1-4244-8046-3.

[2] E. Dvorsky, L. Rakova, P. Hejtmankova, "Primary and secondary frequency regulation with photovoltaic generators", *16th International Scientific Conference on Electric Power Engineering (EPE)*, Kouty nad Desnou, pp. 174-178, May 2015.

[3] D. Zhao, N. Zhang, Y. Liu, "Micro-grid connected/islanding operation based on wind and PV hybrid power system", *IEEE Innovative Smart Grid Technologies - Asia (ISGT Asia)*, Tianjin, pp. 1-6, May 2012, ISBN 978-1-4673-1221-9.

[4] A. Hoke, E. Muljadi, D. Maksimovic, "Real-time photovoltaic plant maximum power point estimation for use in grid frequency stabilization", *IEEE 16th Workshop on Control and Modeling for Power Electronics (COMPEL)*, Vancouver, pp. 1-7, July 2015.

[5] Y. Liu, H. Xin, Z. Wang, D. Gan, "Control of virtual power plant in microgrids: a coordinated approach based on photovoltaic systems and controllable loads", IET Generation, Transmission & Distribution - Special Issue on Power Electronic Converter Systems for Integration of Renewable Energy Sources, Vol. 9, Iss. 10, pp. 921-928, ISSN 1751-8687.

[6] S.T. Cha, H. Zhao, Q. Wu, A. Saleem, J. Ostergaard, "Coordinated control scheme of battery energy storage system (BESS) and distributed generations (DGs) for electric distribution grid operation", *IECON 2012 - 38th Annual Conference on IEEE Industrial Electronics Society*, Montreal, pp. 4758-4764, October 2012, ISBN 978-1-4673-2419-9.

[7] M. Chamana, B.H. Chowdhury, "Droop-based control in a photovoltaic-centric microgrid with Battery Energy Storage", *North American Power Symposium (NAPS)*, Manhattan, pp. 1-6, September 2013.

[8] S. Matsushita, K. Yukita, Y. Goto, K. Ichiyanagi, H. Aoki, Y. Mizutani, "Automatic generation control using GA considering distributed generation", *IEEE/PES Transmission and Distribution Conference and Exhibition 2002: Asia Pacific*, Vol. 3, pp. 1579-1583, October 2002, ISBN 0-7803-7525-4.

[9] E.J. Ng, R.A. El-Shatshat, "Multi-microgrid control systems (MMCS)", *2010 IEEE Power and Energy Society General Meeting*, Minneapolis, pp. 1-6, July 2010, ISBN 978-1-4244-6549-1.

[10] D. Corne, M. Dissanayake, A. Peacock, S. Galloway, E. Owens, "Accurate localized short term weather prediction for renewables planning", *2014 IEEE Computational Intelligence Applications in Smart Grid (CIASG)*", Orlando, pp. 1-8, December 2014.

[11] "Network Code on Requirements for Grid Connection Applicable to all Generators," European commission draft regulation, https://www.entsoe.eu/Documents/Network%20codes%20documents/NC%20RfG/draft_ec_networkCodesJune.pdf, 2015.

[12] S. Lie J. Ma, "Energy control strategy of photovoltaic power station*,*" *IEEE International Conference on Computer Science and Automation Engineering* (CSAE), 2012, vol. 2, pp. 426-430, 2012.

[13] R. Teodorescu, M. Lissere, P. Rodriguez, "Grid converters and photovoltaic and wind power systems, " WILEY, 2011, ISBN 978-0-470-05751-3.

[14] L. Ries, K. Malý, Z. Pavlíček, J. Bízik, "Teoretická elektroenergetika II, " ALFA/SNTL Bratislava 1979.

[15] M. Latkova, P. Bracinik, M. Bahernik, F. Susko, "Modeling of a DC Boost Converter Behavior in PV System Using Finite State Machines," *16th Interantional Scientific Conference on Electrical Power Engineering 2015,*pp.: 733-738, ISBN 978-1-4673-6787-5 .

[16] K. Máslo, "Řízení a stabilita elektrizační soustavy, " Praha, 2013.

[17] P. Mastny, J. Moravek, J. Drapela, "Practical Experience of Operational Diagnostics and Defectoscopy on Photovoltaic Installations in the Czech Republic." Energies 8, no. 10, pp: 11234-11253, ISSN 1996-1073.

[18] "Technické podmienky pre pripojenie a prístup k prenosovej sústave (Grid Code defined by the Slovak TSO)", http://www.sepsas.sk/seps/Dokumenty/TechnickePodmienky/2015/01/01/TP-B_2014.pdf, 2014.